

Enhanced Teleoperation for D&D

Young S. Park, Hyosig Kang, Thomas F. Ewing
Nuclear Engineering Division
Argonne National Laboratory
Argonne, IL, 60439-4803, USA
ypark@anl.gov

Eric L. Faulring, J. Edward Colgate, Michael A. Peshkin
Department of Mechanical Engineering
Northwestern University
Evanston, IL 60208-3111, USA
colgate@northwestern.edu

Abstract—Remote systems will be essential for reducing risk to human workers from hazardous radiation and difficult work environments, while improving productivity and reducing costs. The major drawback of currently available remote manipulator system is that teleoperation is slow and imprecise. The presented work focuses on enhancing remote operation of tools for D&D tasks by introducing teleautonomy and telecollaboration. In teleautonomy, the robot performs a given task autonomously, while human operator intervenes the process as a supervisor. In telecollaboration, the human operator is passively constrained by a virtual fixture, but is responsible for the motion. This work, sponsored by US Department of Energy (DOE) Environmental Management Science Program (EMSP), builds on a reactive, agent-based control architecture and cobot control technology.

Keywords – teleoperation, teleautonomy, telecollaboration, D&D, reactive behaviors, virtual fixture

I. INTRODUCTION

The liability for deactivation and decommissioning (D&D) of contaminated structures in the weapons complex is about \$30 billion. Remote systems will be essential for this work to reduce risk to human workers from hazardous radiation and difficult work environments, while improving productivity and reducing costs. Nevertheless, the major drawback of currently available remote manipulation systems is that teleoperation is a slow and imprecise process, mainly due to the poor visual display. This was evident in ANL's experiences of deploying the teleoperated Dual Arm Work Platform (DAWP) system for dismantling the CP-5 reactor internals at Argonne National Laboratory. Despite significant improvements in productivity using robots over baseline (manual) methods, it was observed that most of the robot operation time was spent in alignment operations, with the remaining time spent performing actual dismantling operations. Also, since the operation of the robot relies solely on human perception-action, precise motions easily achievable by the robot in programmed control become extremely difficult under teleoperation. What is required is a powerful aid that can effectively guide the operator through desired task motions. To this end, this paper presents an enhanced remote manipulator system, which demonstrate efficient and precise teleoperation for the general D&D tasks. Specifically, in this paper, two types of enhanced teleoperation are explored: tele-autonomy and tele-collaboration. In teleautonomy, the robot executes autonomous behaviors, while human operator intervenes the process as a supervisor – sort of

a 'cruise controlled'. In telecollaboration, the operator's motion is passively constrained to a virtual fixture, but the operator feels and controls the progress of what is happening at the same time.

II. SYSTEM DEFINITION

In teleoperation, a human operator looks at video displays, and operates remotely located slave robot via a hand controller. An enhanced teleoperation system, improved for more efficient task performance, is depicted as in Fig. 1. Here, two types of enhancements are the depicted as 'tele-autonomy' and 'tele-collaboration' are described. In teleautonomy, the robot executes reactive behaviors to autonomously perform a task, while human operator intervenes the process as a supervisor providing rough motion trajectory with unilateral input device. In telecollaboration, the reactive behaviors as for teleautonomy might be available; however, instead of being functions of time, the behaviors become functions of spatial parameters. The difference is analogous to a "path" being spatial and a "trajectory" being temporal. For example, in telecollaboration, the operator's motion might be constrained to a particular path, but the motions or forces along that path are determined by the operator. Therefore, the operator feels and controls the progress of what is happening at the same time.

A. Reactive Robotic Architecture

Tele-autonomy is achieved by blending human oversight with sensor-based autonomous operation, forming a semi-autonomous system. The autonomy can be implemented based on either deliberative or reactive architecture. The deliberative architecture is well suited for structured and highly predictable environments, but it lacks the flexibility to cope with uncertain

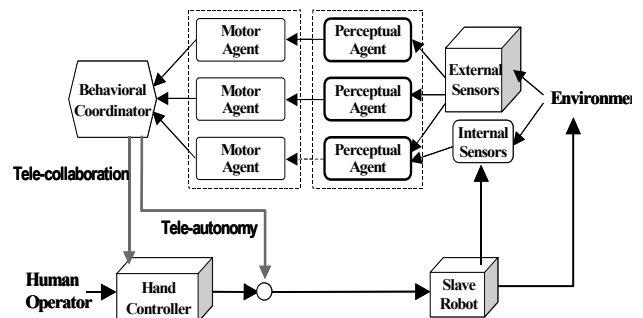


Figure 1. Structure of enhanced teleoperation system

and unstructured environments. On the other hand, a *reactive system* is composed of a collection of behaviors that tightly link sensory inputs to motor actions. The flow of control and communication between each behavior is less restrictive, and autonomous control emerges from the interaction of multiple behaviors. A reactive system is more suitable for autonomy in unstructured and uncertain environment. Furthermore, due to its distributed nature, it exhibits incremental competency - more complex behaviors can be built and tested incrementally from elementary behaviors.

In our implementation, a reactive system is composed of motor agents that directly correlate sensory inputs to the manipulator's motor actions. As shown in Fig. 1, the robot motion is determined as emergent response of multiple motor behaviors. Embedded within each motor agent is a perceptual agent that provides the perceptual information customized for the respective motor behavior.

B. Sensory System

Both forms of enhanced teleoperation require simple and effective environmental sensing. To this end, the use of structured light systems is proposed to form sensory basis. A structured light system is composed of a camera and a patterned beam projector placed in parallel at a known baseline distance, as shown in Fig. 2. By projecting a beam of known geometry, the stereo correspondence problem is simplified. The shape and location of the projected grid pattern can be analyzed to characterize the pose and shape of an environmental object. Projection of patterned beam can also provide effective visual reference for the human operator during teleoperation.

To support diverse sensing strategies, multiple structured light systems are installed at multiple vantage locations of the platform base, wrist points of the robot arms, and on the tools, as depicted in Fig. 3. For instance, different configurations may be selected to avoid occlusions, or to get a closer look. Using the multiple structured light systems, pose measurement involves the following operations: 1) 3-D range measurement using structured light system, 2) online estimation of extrinsic parameters relating the measurement to robot frame, and 3) generation of geometric model and pose estimation.

The 3-D pose measurement is accomplished based on stereo measurement. The intrinsic and extrinsic parameters determined by the structured light system calibration are sufficient to establish the epipolar geometry between the

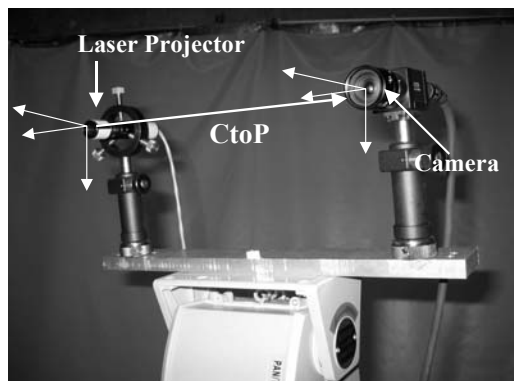


Figure 2. Structured light system

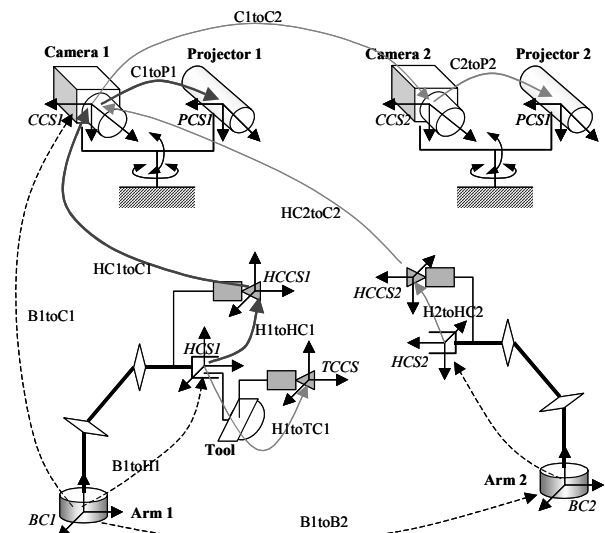


Figure 3. Multiple sensor coordinate frame relationships

camera and the projector. The beam pattern projected onto an object is captured by the camera. Relatively simple image processing and computation is required to identify the grid points. Then, based on epipolar geometry between the camera and the projector, stereo matching is established between the grid points in the camera image and the projector's grid points, as illustrated in Fig. 4(a). The 3-D distance from the camera to the grid points is determined from the disparity between the matching image points. For details of stereovision, refer to O. Faugeras[2]. Fig. 4(b) illustrates a 3-D range map generated for a cylindrical object.

Structured light systems mounted on pan/tilt devices can be driven to point to objects at various locations. Once the object pose is determined with respect to camera frame, call it $CCS1$, it is necessary to relate it to robot base coordinate frame. Referring to Fig. 3, this reduces to determining the kinematic transformation $B1toC1$, which can be expressed as

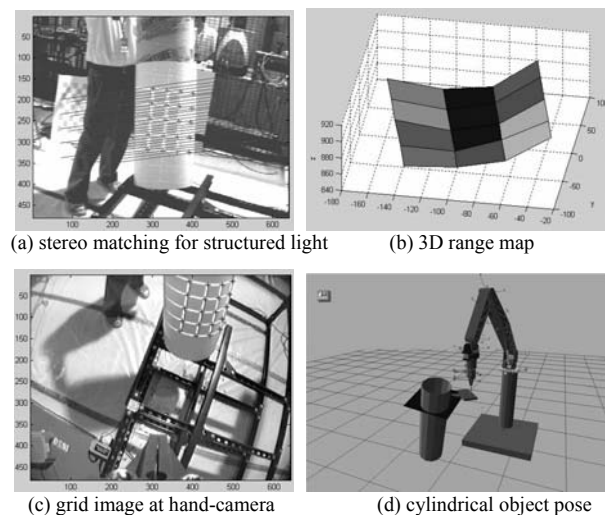


Figure 4. On-line pose measurement with multiple sensors

$$B1toC1 = B1toH1 * H1toHC1 * HC1toC1.$$

Since B1toH1 can be obtained from the robot control system, and H1toHC1 is determined by hand-eye calibration - as in [3], it is necessary to determine HC1toC1, which is the geometric relationship between the hand camera and the structured light sensor. Ordinarily, this is equivalent to the baseline calibration in a stereovision system, which is usually done offline. In our cases, however, the sensors and robots are in frequent motion, and it is necessary to re-establish the extrinsic baseline parameters at every moment. Therefore, an on-line extrinsic parameter estimation technique is devised that relates a structured light sensor and a robot's hand-eye camera. When structured light system takes a measurement, the grid image is captured at the same time by the hand camera, as illustrated in Fig. 4(c). From the array of 3-D object point locations, call it X_c , and the matching point positions in the hand camera image, x_{hc} , nonlinear optimization is carried out to determine the relative locations between the two camera frames. Given a priori information on general shape of the object geometry, the range data are used to estimate the size and orientation of a cylinder, as illustrated in Fig. 4(d). Taking the range data, the perceptual agents generate the perceptual information on need-to-know basis, as described in the following section.

III. TELEAUTONOMY

Our experience in robot operations revealed that most D&D tasks are composed of a few large-grain motor behaviors, namely *inspection*, *move_to_goal*, and *apply_tool*, as shown in Fig. 5. Such high-level behaviors can be assembled from a few primitive motor agents. The characteristics of these motor behavioral assemblages are described as follows:

A. Move_to_goal behavior

Move_to_goal moves the end-effector to a goal location. This behavior provides preliminary motions in between various tasks, which require transporting the tools. As shown in Fig. 6, it is constituted by a sequencing the actions of the following three motor agents:

gross_move_forward: Whenever the presence of a certain

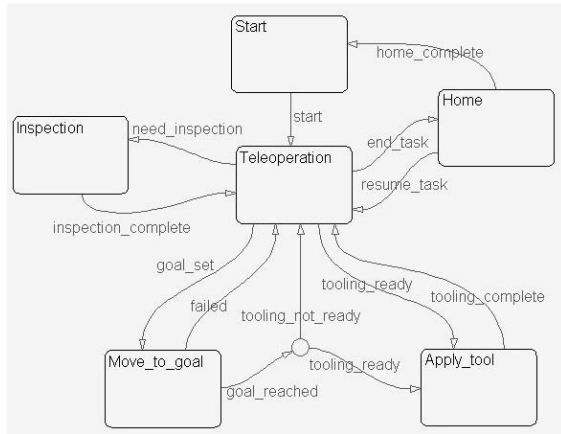


Fig. 5. State-transition diagram for D&D operation

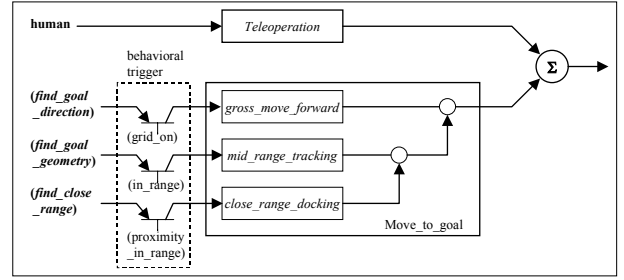


Figure 6. Move_to_goal behavior

landmark pattern is recognized, the robot will move the end-effector move toward the landmark.

mid_range_tracking: This behavior is triggered whenever the presence of a certain landmark pattern is recognized and the distance to the landmark is within a certain range. The robot will move the end-effector toward the landmark, while aligning the end-effector orientation in accordance with the geometric shape of the target work piece. Also, the trajectory is further modified to avoid obstacles.

close_range_docking: When the robot is too close to the target work piece, the camera system is no longer useful. When this condition is recognized, the robot moves its end-effector slowly in the surface normal direction of the work piece until the end-effector touches the work piece.

B. Apply_tool behavior

Apply_tool behavior generates the actions that assist in tool applications. Fig. 7 illustrates the various motor agents constituting *apply_tool* motor behavior. Taking the environmental information from the perceptual schema, the motor schema has as output motion $\dot{\mathbf{x}}$,

$$\dot{\mathbf{x}} = \begin{bmatrix} \mathbf{v} \\ \boldsymbol{\Omega} \end{bmatrix}.$$

where $\mathbf{v} = [v_x, v_y, v_z]$ is translational velocity, and $\boldsymbol{\Omega} = [\omega_x, \omega_y, \omega_z]$ is rotational velocity of the end-effector. These motor actions are encoded in mathematical function. In this work, the reactive motor behaviors are generally described as magnitude and direction, as following.

Teleoperation, $\dot{\mathbf{x}}_{tele}$, allows the human operator to provide internal bias to the control system. This behavior is encoded as

$$\mathbf{v} = k_v \mathbf{v}_m \text{ and } \boldsymbol{\Omega} = k_\Omega \boldsymbol{\Omega}_m$$

where \mathbf{v}_m and $\boldsymbol{\Omega}_m$ denotes the motion command given by the human operator, and k_v and k_Ω are the motion scale factors between master input devices and slave manipulators.

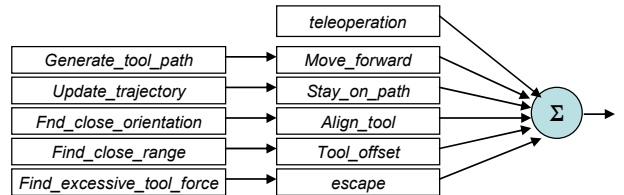


Figure 7. Apply_tool behavior

Move_forward, $\dot{\mathbf{x}}_{\text{move}_f}$, moves the tool at a constant speed along a path generated from an interpretive perceptual schema, *generate_tool_path*. This behavior is encoded as

$$\mathbf{v} = V_{\text{move}_f} \cdot \mathbf{v}_{\text{path}} \quad \text{where} \quad \mathbf{v}_{\text{path}} = \frac{\mathbf{p}_{\text{next}} - \mathbf{p}(t)}{|\mathbf{p}_{\text{next}} - \mathbf{p}(t)|}$$

$$\boldsymbol{\Omega} = W_{\text{move}_f} \cdot \mathbf{w}_{\text{path}} \quad \text{where} \quad \mathbf{w}_{\text{path}} = \frac{\boldsymbol{\delta}_{\text{next}} - \boldsymbol{\delta}(t)}{|\boldsymbol{\delta}_{\text{next}} - \boldsymbol{\delta}(t)|}$$

where V and W are magnitudes, and \mathbf{v}_{path} and \mathbf{w}_{path} are the directional unit vectors denoting translational and orientational from the current tool location to the next location in path. Also, \mathbf{p} and $\boldsymbol{\delta}$ denote position and orientation vectors respectively.

Stay_on_path, $\dot{\mathbf{x}}_{\text{path}}$, provide bias to path following motion to maintain offset distance away from or into the surface.

$$\mathbf{v} = V_{\text{path}} \cdot \mathbf{n}_{\text{path}} \quad \text{where} \quad V_{\text{path}} = W_{\text{max}} \cdot \frac{d}{S}$$

where d is distance of tool to center of path, S is a constant denoting the radius of sphere of influence, \mathbf{n}_{path} is the directional unit vector along a line from tool center to center of path heading toward centerline.

Align_tool, $\dot{\mathbf{x}}_{\text{align}}$, places and orients the tool in the direction normal to the object surface. This is encoded as

$$\boldsymbol{\Omega} = W_{\text{align}} \cdot (\mathbf{n} \times \mathbf{n}_d + \mathbf{o} \times \mathbf{o}_d + \mathbf{a} \times \mathbf{a}_d),$$

$$\text{where} \quad W_{\text{align}} = \begin{cases} 0 & \text{for } d > S \\ W_{\text{max}} \cdot \frac{d}{S} & \text{for } d \leq S \end{cases}$$

$[\mathbf{n}, \mathbf{o}, \mathbf{a}]$ and $[\mathbf{n}_d, \mathbf{o}_d, \mathbf{a}_d]$ are unit vectors denoting current and desired tool orientations.

Tool_offset, $\dot{\mathbf{x}}_{\text{offset}}$, provide bias to the path following motion to maintain offset distance away from or into the surface.

$$\mathbf{v} = V_{\text{offset}} \cdot \mathbf{a} \quad \text{where} \quad V_{\text{offset}} = \begin{cases} 0 & \text{for } d > D + S \\ W_{\text{max}} \cdot \frac{d - D}{S} & \text{for } d \leq D + S \end{cases}$$

where \mathbf{a} is the end-effector approach vector, D is the desired offset distance.

Escape, $\dot{\mathbf{x}}_{\text{escape}}$, moves the tool in backward biased random directions to escape from a jammed condition. This is encoded

$$\mathbf{v} = V_1 \cdot \mathbf{e}_{\text{random}} - V_2 \cdot \frac{\mathbf{v}_{\text{path}}}{|\mathbf{v}_{\text{path}}|}$$

$$\boldsymbol{\omega} = W \cdot \mathbf{e}_{\text{random}}$$

where V_1 and V_2 and W are velocity gains, and $\mathbf{e}_{\text{random}}$ is a unit vector generated in random directions.

C. Experimental operation

Circular saw is a popular D&D tool commonly used for sectioning nuclear reactor walls and pipes. Its operation requires precise alignment and reinsertion of tool blade, as well as forward motion in the cutting direction. During a previous demonstration, its manipulation was proven inefficient with manual teleoperation of DAWP. To demonstrate the improvement under tele-autonomy, an experimental operation is performed for cutting along the circumference of a large pipe, a common structure encountered during D&D. Fig. 8 shows the cutting tool paths for both manual teleoperation and enhanced teleoperation with the assistance of *apply_tool* behavior. The reactive behaviors were proven particularly effective for maintaining tool path and configuration during the circumferential cutting. The operational results revealed that teleautonomy resulted that precise cutting was accomplished in shorter time. Furthermore, the remote operation does not required experienced operator, which is costly to train and difficult to find.

IV. TELECOLLABORATION

Tele-collaboration is another enhanced form of teleoperation addressed in this work. In telecollaboration, the same motor behaviors as for teleautonomy might be available; however, instead of being functions of time, the behaviors become functions of spatial parameters, thus forming *virtual fixtures*.

A. Virtual Fixture

Virtual Fixtures are defined, according to [8], as "abstract percepts overlaid on top of the reflected sensory feedback from a remote environment such that a natural and predictable relation exists between an operator's kinesthetic activities

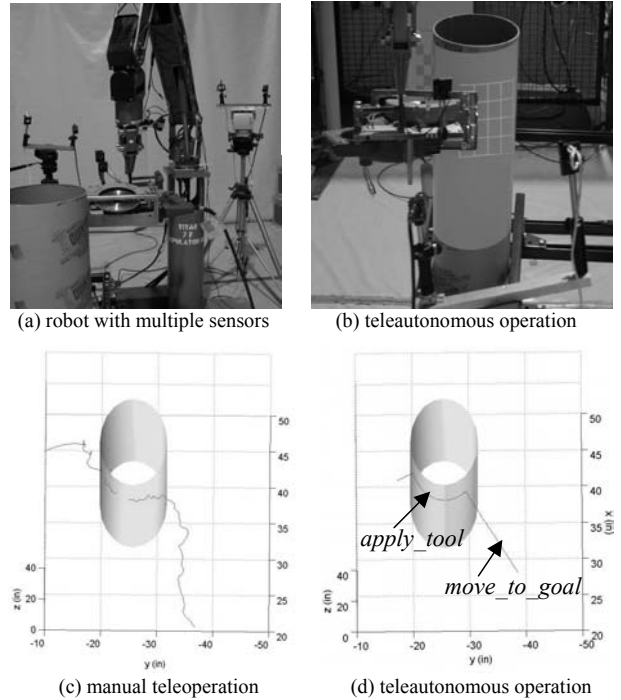


Figure 8. Tool trajectories during teleoperation

(efference) and the subsequent changes in the sensations presented (afference)”. A familiar conceptual model with which to understand the concept of a virtual fixture is a straightedge. Consider using a pencil to draw a straight line on a piece of paper. The straightedge is a physical fixture that may be overlaid to simplify the task. Virtual fixtures may, like the straightedge, provide force feedback, or they may take other forms, such as visual or auditory display.

Likewise, in this work, virtual fixture is implemented to simplify the placing a tool on the target objects while keeping alignment. The type of virtual fixture used in this experiment is a virtual tunnel to guide the cutting tool into the target pipe during the approach phase. The virtual tunnel is defined with radius ε_s at the start position p_s , ε_f at the end position p_f , and the tunnel axis $n_t = p_f - p_s$. A cubic function can be used to determine the tunnel radius ε_t representing how to tolerate the translational deviation from the desired approach trajectory. The tunnel radius ε_t at a given $t \in [0, 1]$ is defined as

$$\varepsilon_t(t) = \varepsilon_f + (\varepsilon_s - \varepsilon_f)(2t^3 - 3t^2 + 1).$$

As approaching the target position, the virtual tunnel shrinks so that the operator can easily guide the position of tool. The virtual tunnel can be only used to assist the translational guidance. In order to assist the operator to align the tool orientation, a virtual aligning cone is created. The virtual cone can be represented as having its vertex at the origin of the tool frame, the axis vector \mathbf{a} aligned the desired direction vector \mathbf{r}_d , and angle α . Since \mathbf{a} is aligned with \mathbf{r}_d , the virtual cone angle α represents how to tolerate the rotational deviation from the desired direction vector. Hence, the operator can get the intuitive perception of the desired rotational motion from this geometrical guidance. Virtual cone can be concisely represented with the introduction of quaternion. With the given start orientation \mathbf{q}_s and the target orientation \mathbf{q}_f , the spherical linear interpolation of quaternion at $t \in [0, 1]$ yields

$$\mathbf{q}_t(t, \mathbf{q}_s, \mathbf{q}_f) = (q_0, \mathbf{q}) = \{\sin((1-t)\theta)\mathbf{q}_s + \sin(t\theta)\mathbf{q}_f\} / \sin(\theta),$$

where $\theta = 2\cos^{-1}(\mathbf{q}_s \cdot \mathbf{q}_f)$. Thus, the centered normal axis vectors of three virtual cones is defined with orthonormal directional vectors from the following equivalent rotation matrix,

$$\mathbf{R} = [\mathbf{r}_{1d} \ \mathbf{r}_{2d} \ \mathbf{r}_{3d}] = \mathbf{I} + (\sin\phi)\mathbf{S} + (1-\cos\phi)\mathbf{S}^2,$$

where $\phi = 2\cos^{-1}(q_0)$ and $\mathbf{S} = (\mathbf{q}/\|\mathbf{q}\|)^\wedge$. Fig. 9 shows the tool side view of the virtual tunnel and cones.

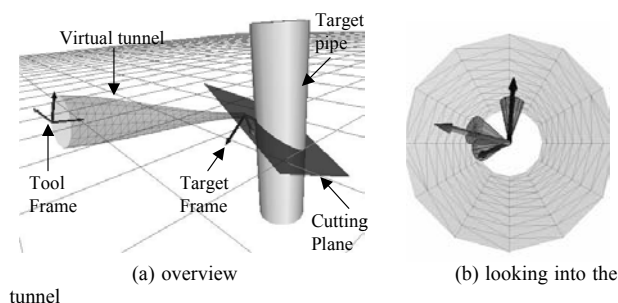


Figure 9. Virtual fixture for circular saw operation

B. A. Cobot Hand Controller

To effectively display the virtual fixture kinesthetically, a new hand controller is developed, based on Cobot technology. Cobot is a proprietary technology capable of providing safe and smooth yet extremely strong constraints through the use of non-holonomic constraints[9-11]. A steered wheel, un-powered about its rolling axis, creates a relationship between the two components of its linear velocity. Higher dimension cobots utilize varying geometries of rolling contacts. Cobots can either be operated in “free-mode,” where the intent of the operator in the full dimension of the task space is followed completely, or in “virtual-surface” mode, where a lower dimensional surface than the task space guides the operator’s intent tangent to that surface, and the non-holonomic constraints of the rolling wheels, not the torque of any actuators, prevent motion normal to the virtual surface.

The design of this 6-DOF Cobot Hand Controller utilizes the kinematics of a parallel platform introduced by Merlet[11] (Fig. 10 and 11). The proximal links are coupled by three degree-of-freedom universal joints to the distal links, and these in turn are coupled via two degree-of-freedom universal joints to an end-effector platform. A force sensor on the end-effector is used to determine the user’s intent. Our addition to Merlet’s kinematics has been to couple the six linear actuators to a central “power cylinder” through non-holonomic constraints. Linear actuation of the proximal links is achieved via a rotational to linear continuously variable transmission (CVT), namely a steered wheel. The angle of each wheel relates the linear velocity v_i of each proximal link to the rotational velocity of the power cylinder ω . When the wheels are steered such that their rolling axis is parallel to the power cylinder ($\phi_i = 0$), a ratio $v_i / \omega = -r \tan(\phi_i) = 0$ is set. If the wheels are steered either direction from $\phi_i = 0$, ratios between \pm infinity can be achieved. In practice, wheel slip limits this range. It is also evident, that turning all six wheels to $\phi_i = 0$ locks the six actuators, and turning them to $\phi_i = \pi/2$ completely decouples the actuators from the cylinder’s velocity, although the cylinder would then be unable to turn.

As mentioned before, an operator can interact with the cobot in a “free mode” in the full dimensional six-space, or while constrained to a one to five dimensional virtual-surface. In Fig. 12, a trajectory on a four-dimensional constraint surface is shown. The user’s force input in two dimensions is followed via a mass-damping model. The operator is constrained to zero rotation about all three axes, and to the surface of a 17 cm

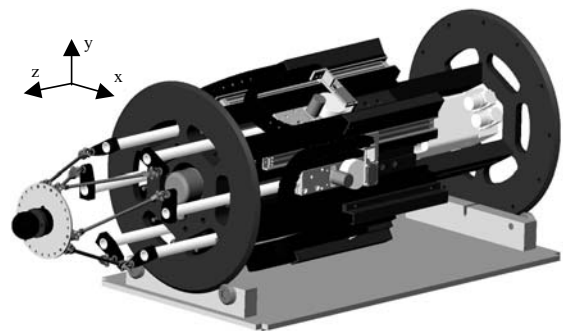


Figure 10. A CAD model of the 6-DOF Cobot Hand Controller

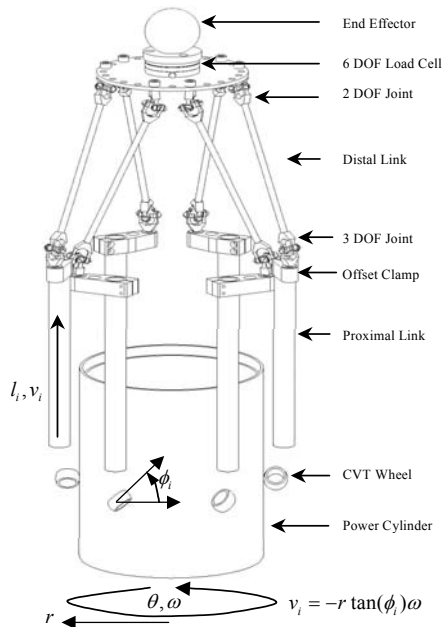


Figure 11. The kinematics of a Merlet-Cobotic parallel platform

diameter sphere, which provides a good representation of the available translational workspace. At the center of the Cobotic Hand Controller's translational workspace, ± 40 degree rotations about x, ± 45 degree rotations about y, and ± 85 degree rotations about z are feasible.

The test operation revealed that active six-degree-of-freedom Cobotic haptic display with workspace resolution of approximately $25 \mu\text{m}$, force transmission capabilities exceeding 50 N, structural stiffness ranging from 20-400 kN/m. Based on the authors' experience with haptic interface devices, the feeling of this device is quite remarkable. The crisp distinction between free and forbidden directions of motion is striking. This performance arises not from elaborate control algorithms, but from the inherent physical characteristics of the device due to the utilization of non-holonomic constraints.

V. CONCLUSION AND FURTHER STUDIES

To aid in teleoperation of D&D tool manipulation, two types of enhanced teleoperation technologies are developed, namely teleautonomy and telecollaboration. The technology, built upon reactive robotic architecture and Cobot technology, involves comprehensive development of sensory basis, robot control system and virtual fixture. Both types of enhanced teleoperation serve a useful role. Tele-autonomy is particularly useful for routine operations where the operator does not require sensory feedback. Tele-collaboration may be more useful for situations where the operator needs such feedback, such as feeling the vibration from the saw cutting action to guard against binding. Preliminary experimental studies revealed effectiveness of each method. A synergistic advantage can be achieved by combining both tele-autonomy and tele-collaboration. The choice between the two must ultimately be related to the quality of sensory information available to

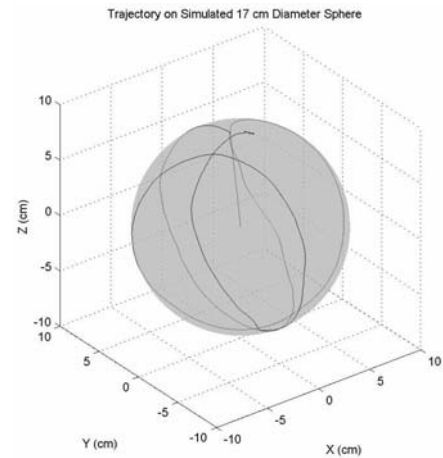


Figure 12. Average tangential force on the user during exploration of the sphere was 0.5 N. Approximately half of this was intentionally due to simulated mass and damping.

computer controller, versus that available to the human operator. More work is expected in this area.

ACKNOWLEDGMENT

This research was sponsored by the Environmental Management Science Program of the Office of Environmental Management, U. S. Department of Energy.

REFERENCES

- [1] R. C. Arkin, "Reactive Control as a Substrate for Telerobotic Systems," *IEEE Aerospace and Electronics System Magazine*, Vol. 6, No. 6, pp. 24-31, June, 1991
- [2] O. Faugeras, *Three-Dimensional Computer Vision: A Geometric Viewpoint*, MIT Press, 1993
- [3] Y.C. Shiu and S. Ahmad, "Calibration of wrist-mounted robotic sensors by solving homogeneous transformation equations of the form $AX=XB$ " *IEEE Trans. Robotics Automat.*, vol. 5, pp.16-29, 1989
- [4] C. Wang, "Extrinsic calibration of a vision sensor mounted on a robot" *IEEE Trans. Robotics Automat.*, vol. 8, pp.161-175, 1992
- [5] Park, Y.S., Boyle, J.M., Ewing, T.F., "Agent Based Dual-arm Motion Planning for Semi-automatic Teleoperation," *Proc. of ANS 9th International Topical Meeting on Robotics and Remote Systems*, Seattle, Washington, March 4-8, 2001
- [6] Y. Park, "Structured beam projection for semi-automatic teleoperation," *Proc. of SPIE 2000 ISAM Conference on Opto-Mechatronic Systems*, Boston, MA, Nov. 5-6, 2000
- [7] J. V. Draper, and Blair, L.M., "Dual arm work platform performance estimates and telerobot task network simulation," presented at *American Nuclear Society Seventh Topical Meeting on Robotics and Remote Handling*, Savannah, GA, 1997.
- [8] L. B. Roseberg, "Virtual fixtures: perceptual overlays enhance operator performance in telepresence tasks," in *Mechanical Engineering: Stanford University*, 1994.
- [9] M. A. Peshkin, Colgate, J.E., Wannasuphprasit, W., Moore, C.A., Gillespie, R.B., and Akella, P., "Cobot architecture," *IEEE Transactions on Robotics and Automation*, vol. 17, pp. 377-390, 2001.
- [10] E. L. Faulring, Colgate, J.E., Peshkin, M.A., "A high performance 6-DOF haptic cobot," submitted to *IEEE International Conference on Robotics and Automation*, 2004.
- [11] J. P. Merlet, "Direct kinematics and assembly modes of parallel manipulators," *International Journal of Robotics Research*, vol. 11, pp. 150-162, 1992